Pattern Recognition 43 (2010) 1016–1026

Contents lists available at ScienceDirect

Pattern Recognition

journal homepage: www.elsevier.de/locate/pr

Comparison and combination of iris matchers for reliable personal authentication

Ajay Kumar [a,b,*], Arun Passi [a]

[a] Biometrics Research Laboratory, Indian Institute of Technology Delhi, New Delhi, India
[b] Department of Computing, The Hong Kong Polytechnic University, Hong Kong

ARTICLE INFO

Article history:
Received 29 March 2008
Received in revised form
29 June 2009
Accepted 19 August 2009

Keywords:
Iris
Biometrics
Personal authentication

ABSTRACT

The personal identification approaches using iris images are receiving increasing attention in the biometrics literature. Several methods have been presented in the literature and those based on the phase encoding of texture information are suggested to be the most promising. However, there has not been any attempt to combine these approaches to achieve further improvement in the performance. This paper presents a comparative study of the performance from the iris authentication using Log-Gabor, Haar wavelet, DCT and FFT based features. Our experimental results suggest that the performance from the Haar wavelet and Log-Gabor filter based phase encoding is the most promising among all the four approaches considered in this work. Therefore, the combination of these two matchers is most promising, both in terms of performance and the computational complexity. Our experimental results from the all 411 users (CASIA v3) and 224 users (IITD v1) database illustrate significant improvement in the performance which is not possible with either of these approaches individually.

1. Introduction

The iris identification has emerged as a preferred modality for large-scale user authentication and has significantly higher user-acceptance as compared to the more reliable retinal identification. The iris patterns are highly stable and unique as the probability for the existence of two irises that are same has been theoretically estimated to be very high, i.e. one in 10^{72} [8]. Although the performances from the iris patterns have been extensively evaluated in the literature, it is often inadequate to meet the rigorous requirement for very large scale applications. The personal identification approaches using multi-biometrics (multi-algorithm, multi-features, multi-classifiers, etc.) are more promising for such applications and are yet to be investigated for performance improvement using iris images.

1.1. Related work and motivation

The iris identification using analysis of the iris texture has attracted lot of attention and researchers have presented variety of approaches in the literature [1–10]. Daugman [2,22] has presented highly accurate 2D Gabor filter based approach for the iris identification system that employed 2048 bit iris-code. He has also presented [21] the most promising experimental results from large-scale *private* database. Boles [5] has detailed fine-to-coarse approximation at different resolution levels that are based on zero-crossing representation from the wavelet transform decomposition. Wildes et al. [7] have focused on efficient implementation of gradient-based iris segmentation using Laplacian pyramid. Proença and Alexandre [8] have suggested region-based feature extraction for the iris images acquired from large distances. Thornton et al. [1] have recently estimated the non-linear deformations from the iris patterns and proposed a Bayesian approach for reliable performance improvement. Huang et al. [20] have demonstrated the usage of phase-based local correlations for matching iris patterns and achieved notable performance over the prior techniques. Ma et al. [4,6] employed multi-scale bandpass decomposition and evaluated comparative performance from prior approaches. They also presented [24] an effective alternative for iris identification using Gaussian–Hermite moments extracted from 1-D iris intensity signals. The compact representation of iris features using moment invariants extracted from the Gabor wavelet features has shown to offer attractive performance and detailed in [22]. Sanchez-Avila et al. [30] have made promising improvement in the method suggested in [5]. Accurate segmentation of iris and eyelash regions is the key for the accurate iris recognition and has been the focus of study in [26,27]. Motivated by the success of minutiae representation commonly employed in fingerprint representation, Yu et al. [28] have attempted to extract key points from iris texture and illustrated promising results.

* Corresponding author. Tel.: +852 2766 7254; fax: +852 2774 0842.
E-mail address: ajaykr@ieee.org (A. Kumar).

0031-3203/$ - see front matter © 2009 Elsevier Ltd. All rights reserved.
doi:10.1016/j.patcog.2009.08.016

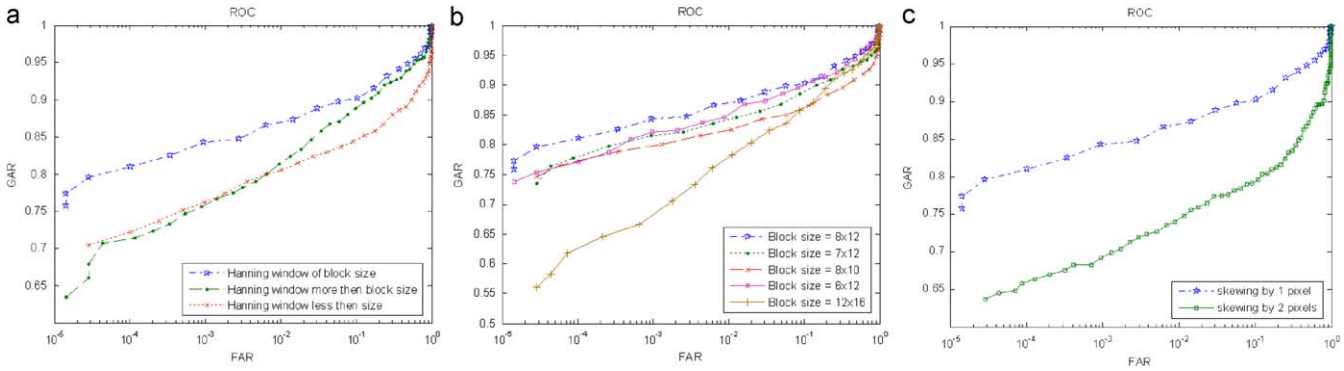

Fig. 1. Selection of block size from the resulting performance using one training in (a) and (b) the corresponding performance from block orientation.

The summary of prior work [25] on the iris identification suggests that there has been very little effort to combine the promising approaches presented in the literature and investigate the performance improvement. It may be noted that such combination should have the merit of improved accuracy and requires relative performance analysis of the candidate approaches. It is generally believed that the acquisition of large number of images for user registration (or for the offline training of biometric system) causes inconvenience to the users and therefore smaller number of training images is always desirable for the performance evaluation. Therefore, the performances from the prior approaches, or from the proposed combination methods, need to be evaluated using minimum[1] training set to ascertain its effectiveness.

2. Our work

The work detailed in this paper [29] focuses on the comparative performance evaluation of the phase encoding of iris patterns using four approaches; Haar wavelet, Gabor filter, Discrete Cosine Transform (DCT), and Fast Fourier Transform (FFT) based feature extraction. The combination of the best performing approaches is used to investigate the further performance improvement. The experimental results detailed in this paper suggest that the performance from the Haar wavelet and Log-Gabor filter based phase encoding is the most promising among all the four approaches considered in this paper. Therefore, simultaneously extracted matching scores from these two matchers are combined to achieve further performance improvement. The prior work in the literature of iris identification approaches illustrated promising performance but with the usage of several training images. Therefore, another objective of this work is to evaluate the comparative performance of various approaches with only *one* training image. The performance from the developed system, using the combination of matchers, is extensively evaluated using *one* training image on publicly available CASIA [15] and IITD database [16].

Our implementation of the considered four approaches is largely based on their details presented in the literature. While evaluating these approaches, various combinations of parameters are attempted, separately for three different databases, to achieve the best possible performance. The performance from the developed online system is evaluated on newly acquired IITD iris image database, which is being made available freely for the researchers. The following Sections 2.1–2.4 briefly describe these matchers and our implementation for the performance evaluation. The image normalization steps involving the segmentation of iris and eyelash regions are detailed in Section 3. The rigorous experimental results from three different iris databases are detailed in Section 4 which is followed by the discussion on the results and the contributions of this paper. Finally the Section 6 summarizes the main conclusions from this paper.

[1] The minimum or one training image performance is of significant interest in the forensic analysis.

2.1. Discrete cosine transform

The iris recognition using the phase information from the zero crossings of the one dimensional DCT has shown promising results in [3]. The DCT coefficients $C(u)$ from the signal $f(x)$ of length L are obtained as follows:

$$C(u)=\varepsilon(u)\sum_{x=0}^{L-1} f(x)\cos\left[\frac{\pi\cdot u}{2\cdot L}(2x+1)\right]\forall u=0,1,\ldots,L-1 \quad (1)$$

where $\varepsilon(u)=2/L$ for $u\neq 0$ and $\varepsilon(u)=2\sqrt{2}/L$ for $u=0$. Our implementation of this approach was iteratively tuned to achieve the best performance (as illustrated from various results in Fig. 1). The skewing of successive rows by one pixel to the right was used to extract the blocks orientated at 45°. Then the weighted average under a $\frac{1}{4}$th Hanning window is performed on each block which reduces the horizontal resolution and the degrading effects of noise and generates a 1D vector. That vector is then windowed using a similar Hanning window in the vertical direction before the application of DCT. Now, difference of adjacent DCT output vectors are calculated and feature vector is formed from their zero crossings. The size of the feature vector depends on the amount of information (bits) retained after the application of DCT. For matching of two iris templates a modified version of hamming distance is used in which the product of sum of respective bits corresponding to each block:

$$S=\left(\prod_{i=1}^{M}\frac{\sum_{j=1}^{N} Block1_{ij}\oplus Block2_{ij}}{N}\right)^{1/M} \quad (2)$$

where M is the number of bits per block in vertical direction, N is the total number of blocks. This method of consolidating the hamming distance can improve the genuine matches by skewing the matching scores S towards zero and also improve the imposter matches by skewing the corresponding scores S towards 0.5 [3]. Fig. 1 illustrates the selection of block size and their orientation (skew) from the achieved performance when only one image was used for the training and rest six images are used for evaluation. The receiver operating characteristics (ROC) in Fig. 1 shows the variation of genuine acceptance rate (GAR) with corresponding false acceptance rate (FAR). The evaluation results shown in Fig. 1 suggest that the block size of 8×12, with overlapping of 4 pixels vertically and 6 pixels horizontally, achieves the best results.

Similarly, these results also suggest that higher performance is achieved when the size of Hanning window is chosen to be equal to the width and height of the corresponding block, and the blocks are oriented at 45° (achieved by skewing of successive rows of the image by one pixel).

2.2. Fast fourier transform

The local frequency variations can also be employed for encoding the phase information from the iris texture. The enhanced iris images are firstly divided into block aligned at 45°. The blocks are then averaged in the horizontal direction and then multiplied by a Hanning window, which results in a 1-D signal corresponding to each block. This signal $f(x)$ is employed to extract the one dimensional FFT coefficients, $F(k)$, as follows:

$$F(k) = \sum_{x=1}^{L} f(x) \exp\left\{\frac{-2\pi j(k-1)}{L}\right\}, k = 1, 2 \ldots, L \quad (3)$$

The difference in the magnitude of adjacent blocks is computed and a binary feature vector is formed from the zero crossings of each difference. The size of the blocks was chosen to be 8×12 with an overlapping of 4 pixels in the vertical direction and 6 pixels in the horizontal direction. The size of the resulting feature vector was 8160 bits and Hamming distance was used to measure the difference between the feature vectors.

2.3. Haar wavelet

The texture details in the iris region can be analyzed at different resolutions using its mulitiscale wavelet decomposition. The Haar wavelets can capture sharp discontinuities in the spatial gray-level texture by repeated application of following low-pass (g) and high-pass (h) filters [9]:

$$g = \frac{1}{\sqrt{2}}[1 \;\; 1], h = \frac{1}{\sqrt{2}}[1 \;\; -1] \quad (4)$$

The above filters are separately applied to the rows and columns of the iris images resulting in four channel filter bank with channels LL, LH, HL, and HH corresponding to filters $g^t g$, $g^t h$, $h^t g$, and $h^t h$, respectively. The recursive application of this decomposition is used to construct higher level decomposition. The feature extraction using the four-level Haar wavelet decomposition [10] of the enhanced image was firstly investigated. The diagonal coefficients of the fourth level were employed to obtain 4×32 real values. In addition to these 128 values, the average of diagonal coefficients from the first, second and third level decomposition were also employed. Each of those 131 (3+128) values were quantized to binary values by simply converting the positive values to 1 and negative values to 0. Therefore, the feature vector for any iris constituted of only 131 bits. The Hamming distance was again employed to match two feature vectors. However, as shown in Fig. 2, the performance from these features was poor and therefore we also investigated performance using higher level wavelet coefficients as suggested in [11].

In this approach, the enhanced images are decomposed into five levels by the Haar wavelets. Next the vertical, horizontal and diagonal coefficients of 4th and 5th level were employed. The coefficients of 1st, 2nd, and 3rd level were almost the same as those of the 4th level and therefore the smallest of them (4th level coefficients) were employed and rest were ignored. The 5th level decomposition offered the most discriminative information and therefore all the coefficients from this decomposition were employed. The phase encoding from the zero crossings of the coefficients formed the binary values of the feature vector. The size of this feature vector was 3 times the size of features of 4th level (4×32) plus 3 times the features of 5th level (2×16), therefore in total the size of feature vector was 480 bits. The Hamming distance was then employed to ascertain the matching distance between feature vectors. The feature vectors are shifted left and right bit-wise and the lowest from the number of hamming distances calculated from successive shifts is employed. The shifting of feature vectors to the left and right by 12 bits can account for the possible rotation of the extracted iris and significantly improved the performance as shown in Fig. 2 (one training image and seven test images per user).

2.4. Gabor filter

The features extracted from the phase encoding of iris texture has gained lot of attention since the fundamental work of Daugman [2]. The response from the bank of 2D Gabor filters can reliably encode the phase information in the iris texture and has shown to offer promising performance. However, the Gabor filters over represent the low frequency components and under represent the high frequency components in any encoding, and an even-symmetric Gabor filter will have a DC component whenever the bandwidth is larger than one octave. Therefore, the Log-Gabor filters have been recently suggested [12,13] for phase encoding because the zero DC-component can be obtained for any bandwidth by using a Gabor filter which is Gaussian on a logarithmic scale. The Log-Gabor filters having extended tails at the high frequency end are expected to offer more efficient encoding of natural images [14]. Fig. 3 shows real and imaginary components of a typical 1-D Log-Gabor filter.

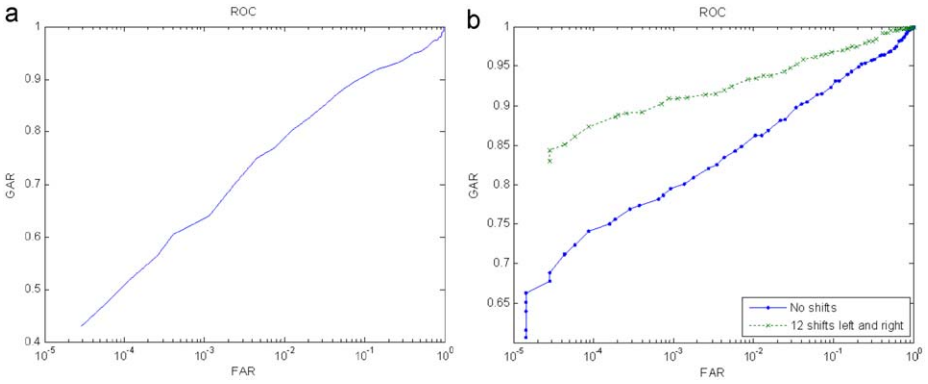

Fig. 2. The performance from the Haar wavelet based approach using 4-level decomposition as detailed in [10] (a) and 5-level decomposition in (b).

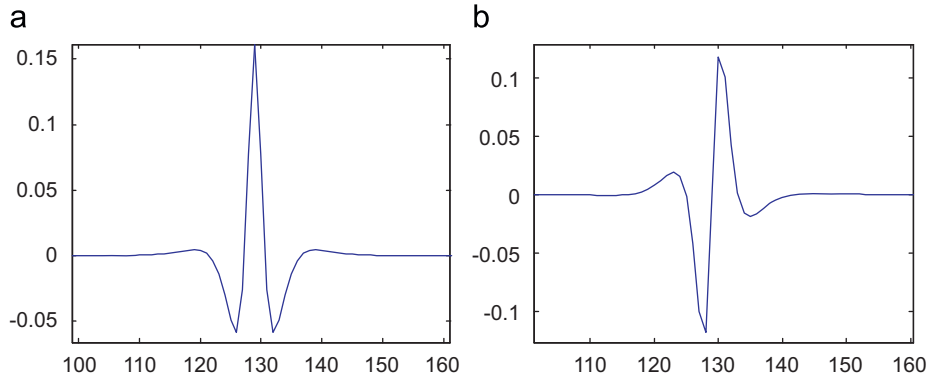

Fig. 3. (a) Real and (b) imaginary Log-Gabor filters in spatial domain having bandwidth of 2 octaves and a center frequency of $\frac{1}{18}$.

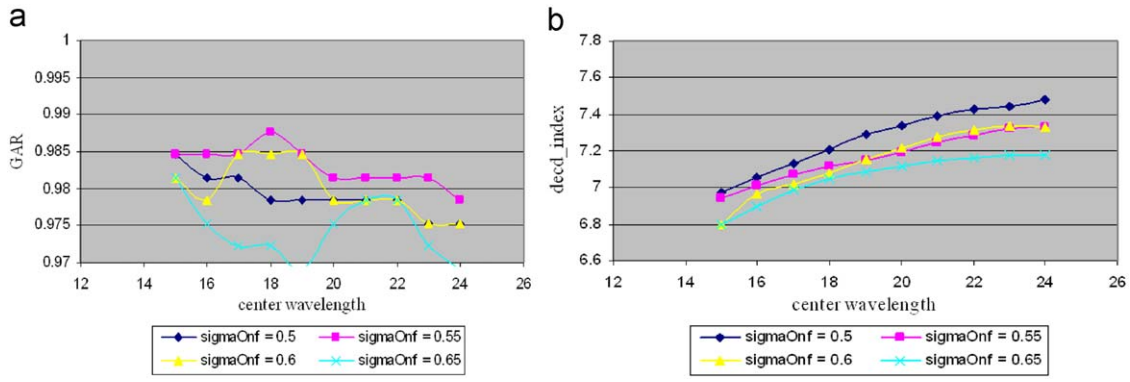

Fig. 4. (a) Variation of GAR at 0% FAR and (b) the decidability index as a function of center frequency and bandwidth of Log-Gabor filter for the CASIA I database.

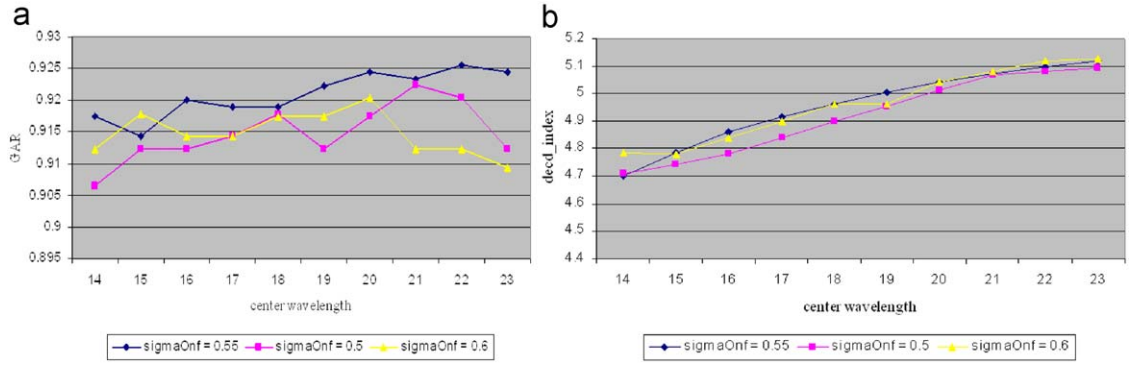

Fig. 5. For CASIA III database and was therefore selected for the entire performance evaluation reported in this paper.

The Log-Gabor function has singularity in the log function at the origin, therefore the analytic expression for the shape of the Log-Gabor filter cannot be constructed in spatial domain. Therefore, the filter is implemented in frequency domain. The frequency response of Log-Gabor filter in frequency domain is defined as follows:

$$G(f) = \exp\left(\frac{-(\log(f/f_0))^2}{2(\log(\sigma_f/f_0))^2}\right) \tag{5}$$

with f_0 is the central frequency and σ_f is the scaling factor of the radial bandwidth B. The radial bandwidth in octaves is expressed as follows:

$$B = 2\sqrt{2/\ln 2}\,|\ln(\sigma_f/f_0)| \tag{6}$$

The parameters for the Log-Gabor filter were empirically selected to achieve the best performance. The decidability index (DI) represents *average* separation of genuine and imposter matching scores and is same as detailed in [22]. However, the optimization of the performance indices obtained from ROC for the most likely operating point of the system (e.g. GAR at 0% FAR) is highly desirable and therefore employed to select the parameters of Log-Gabor filter. The center wavelength of 18 and the ratio σ_f/f_0 (sigmaOnf) of 0.55 achieves the best performance as shown in Fig. 4 and was therefore employed for CASIA I database. Similarly the center wavelength of 22 and σ_f/f_0 equal to 0.55 can achieve best performance as shown in Fig. 5 for CASIA III database and was therefore selected for the entire performance evaluation reported in this paper.

3. Preprocessing and normalization

The entire steps for the extraction of normalized iris regions from acquired images were iteratively refined and were efficiently implemented for the online identification. The pupil in the

acquired image usually contains reflection from the illumination source, which forms some bright spots in the pupil, so if the pixel value inside the pupil is over a particular threshold (200) then it is replaced by pixel value of some neighborhood pixel. This operation almost fills the circles but this still it is not good enough to apply a global threshold for the pupil circle estimation. Therefore, as shown in Fig. 6, resulting images are further subjected to a 7×7 median filter.

The pupil in the resulting images usually appears as a highly distinct black circle. The pupil center in our approach is estimated by scanning the image row-wise and the number of consecutive pixels, whose value is less than certain threshold (say 65 in our implementation), are counted for every row. The row containing the highest number of such consecutive pixels must correspond to the diameter of the pupil, half of that maximum value corresponds to the radius of the pupil, the y coordinate of the center of pupil is the row of the diameter and the x coordinate is calculated by adding radius of pupil to the column from where the consecutive pixels started (Fig. 7). The contrast from the image filtered from the median filter is higher and therefore it is subjected to the Gaussian filtering to remove further noise due to iris texture, then the edge detection is performed using the canny edge detector.

After the edge detection a 20×20 window is chosen in the edge detected image around the center of the pupil. Then every pixel in this window is assumed as the center (candidate centers) and the numbers of white pixels, that are encountered at the perimeter of circle, with radius varying from 80 to 120 pixels, are computed. The winner, i.e., the radius (among 80–120 pixel) and the center (among all 20×20 pixels) for which the maximum white pixels are encountered, is located. That radius R corresponds to the radius of the iris and pixel which was chosen as the center P, which gave that maximum count, is the center of the iris. Although, this method is computationally more expensive then the methods employed in the literature, but, it has been experimentally shown to be far more robust. Therefore, this method was employed for all the experimental results (from the CASIA I, CASIA III, and IITD database) reported in this paper. The response from the involuntary physiological mechanism, to the varying image acquisition conditions, influences the size of the iris images employed for the feature extraction. In our implementation, the stretching of iris texture due to changes in pupil size is compensated by employing the unwrapping model of iris that can remove the non-concentricity of iris and pupil. Fig. 8 shows an unwrapped image sample with eyelashes and the corresponding mask extracted for generating matching scores. Fig. 9 shows the unwrapped (also enhanced) rectangular regions of 48×432 pixels from our acquired image sample in IITD database and Fig. 10 shows the corresponding image sample and its unwrapped region of 64×512 pixels from CASIA III database.

3.1. Combination strategies

The performance improvement in the unimodal biometrics system can be achieved from the combination of multiple samples, multiple sensors and multiple matchers. The acquisition of multiple iris image samples or the acquisition from multiple

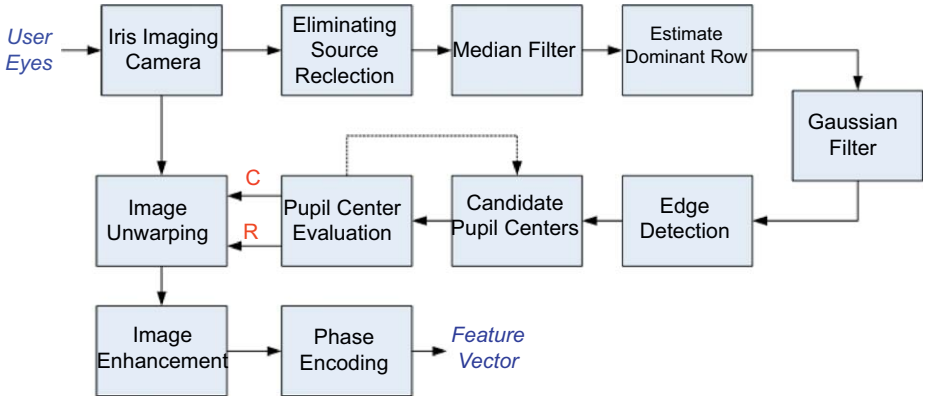

Fig. 6. The image normalization steps in our implementation for iris extraction.

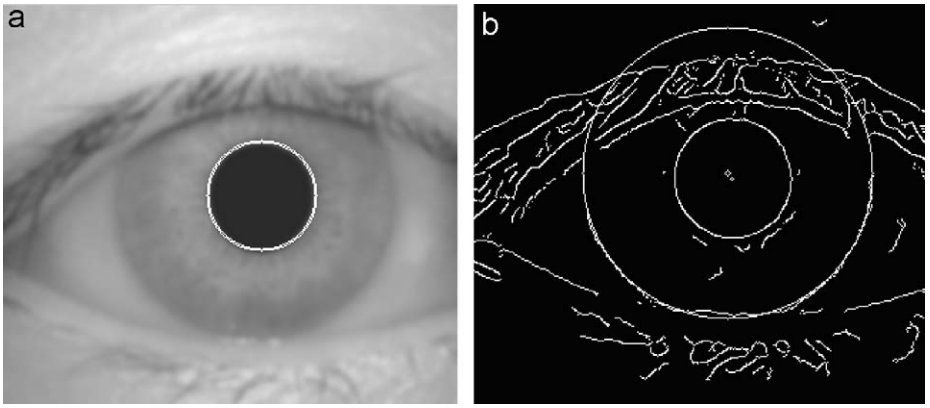

Fig. 7. (a) Estimated pupil from the dominant row and (b) the estimated iris boundary from the candidates centers.

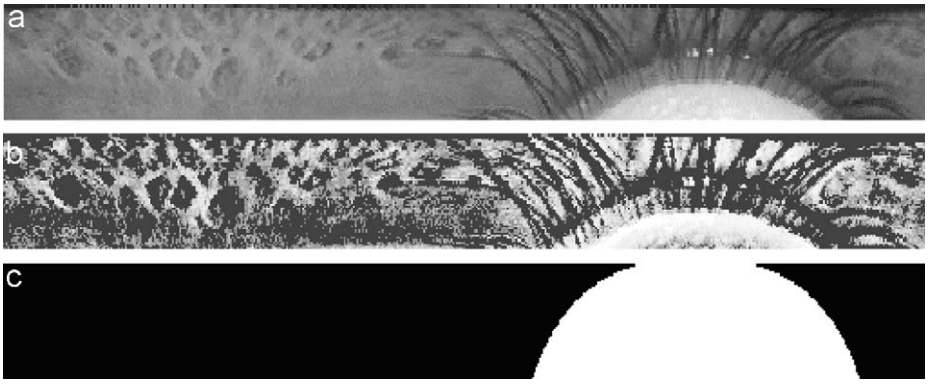

Fig. 8. (a) Unwrapped image, (b) enhanced image, and (c) extracted mask.

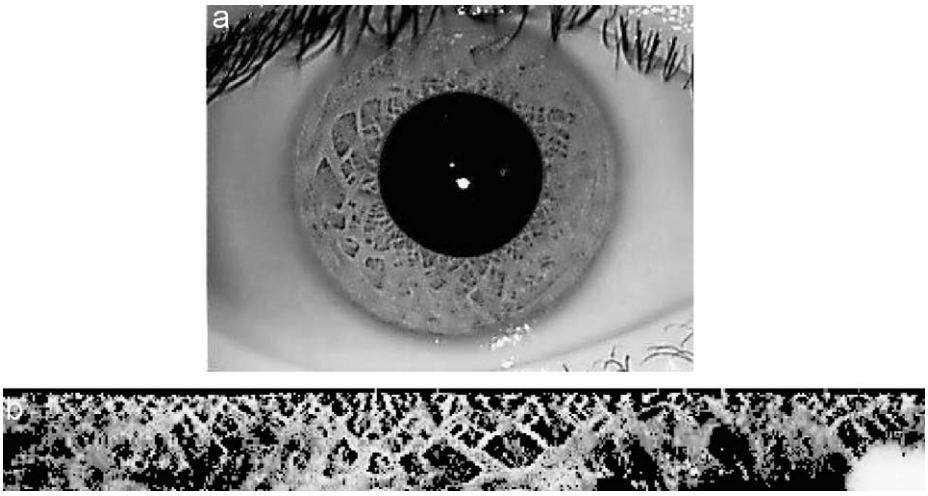

Fig. 9. (a) Acquired 320×240 pixel image from the JIRIS JPC1000 Iris camera in IITD database and (b) the corresponding 432×48 pixels unwrapped enhanced image.

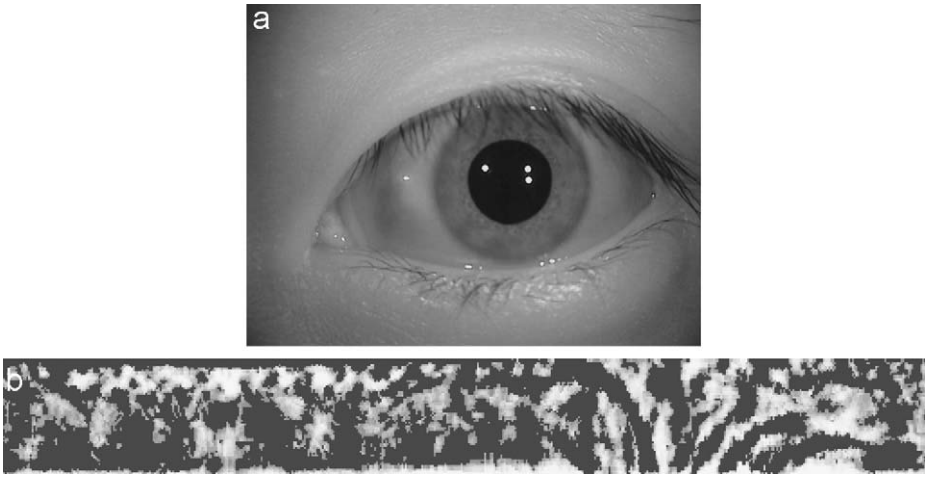

Fig. 10. (a) The 640×480 pixel image from CASIA III database and (b) the corresponding 512×64 pixel unwrapped enhanced image.

sensors highly increases user inconvenience and is therefore not attractive. However, the combination of multiple iris matchers is most promising for online user identification and is therefore investigated in this work. This combination can be typically achieved from the feature-level, matching score-level or the decision-level fusion individual matchers. The phase encoding process employed for the feature extraction, in all the four matchers considered in Section 2, generates binary templates containing bits of information. Therefore, feature-level concatenation of these bit-wise templates cannot exploit temporal information contained in the templates from individual matchers. On the other hand, the matching score-level combination usually achieves better performance than decision-level combination. This is due to the fact that score-level representation has higher information content than the abstract class or decisions. The score-level combination offers best trade-off in terms of

information content and ease in fusion [32]. Therefore, performance improvement using score-level combination of multiple iris matchers is highly promising and investigated in this work.

The combination of matching scores using density-based fusion can offer high accuracy but most complex to implement [31]. In this work, the score-level combination of different iris matchers using fixed fusion rules is employed as they are computationally simple. The combined matching score for every user i, $\forall i=1,2,\ldots,C$, using sum, product and min rule is obtained as follows:

$$m_a(i) = \frac{1}{Z}\sum_{j=1}^{Z} s_{ij} \tag{7}$$

$$m_p(i) = \left(\prod_{j=1}^{Z} s_{ij}\right)^{1/Z} \tag{8}$$

$$m_n(i) = \min_{\forall j}(s_{ij}) \tag{9}$$

where s_{ij} is the individual matching score from ith user using jth matcher, $m_a(i)$, $m_p(i)$, and $m_n(i)$ represents the consolidated matching scores using Sum, Product and Min rule, respectively. The Min rule is expected to perform better while consolidating matching scores having 'outlier' type errors. Ref. [17] suggests the usage of Product rule for the highly independent matchers and Sum rule for the correlated matchers in which case the errors from the individual matchers are independent. In addition to these rules, one can also generate the consolidated matching score $m_w(i)$ from the weighted combination of individual matching scores;

$$m_w(i) = \sum_{j=1}^{Z} w_j s_{ij} \tag{10}$$

where $\sum w_j = 1$ and $w_j \geq 0$. The weights w_j indicate the importance of individual matchers and are estimated during training stage using exhaustive search. The computational complexity of combining matching scores, for online user identification, using above considered fixed combination rules is $O(ZC)$.

4. Experiments and results

The rigorous experiments were performed to select the parameters that can achieve best possible results. We build-up a new *IIT Delhi Iris Database* from the developed online system which mainly consists of the iris images collected from the students and staff at IIT Delhi, India. This database has been acquired in Biometrics Research Laboratory during Jan-July 2007 using JIRIS, JPC1000, digital CMOS camera [19]. The acquired images were saved in bitmap format. The database of 1120 images is acquired from 224 different users and made available freely to the researchers [16]. All the subjects in the database are in the age group 14–55 years comprising of 176 males and 48 females. The resolution of these images is 320×240 pixels and all these images were acquired in the indoor environment.

We firstly report the experimental results from the four matchers employed to ascertain the performance from the CASIA I and CASIA III database which is followed by results from the IITD database. The performance from the four considered matchers significantly varies with the increase in number of training images. Therefore, the experiments were performed to ascertain the performance improvement with varying number of training images.

Fig. 11(a) illustrates the ROC from the DCT based approach detailed in Section 2.1. Similarly, Fig. 11(b) illustrates the ROC from the FFT based approach as detailed in Section 2.2. Significant increase in the performance can be observed with the increase in number of training images while the DCT based approach achieves much better performance as compared to the approach using FFT features. Fig. 12 illustrates individual performance from the Haar wavelet and Log-Gabor filter approach.

The performance from the Log-Gabor filter shown in Fig. 12(b) is observed to be the best among all the four considered approaches, however, its performance does not improve as the number of training images are increased from three to four. This is possibly due to the overtraining from the increase in number of training images. The performance from the FFT based approach (Fig. 11-b) has been the worst among the four considered approaches and therefore this approach was not considered for the score level fusion.

We performed rigorous experiments for the score level combination of best performing three approaches using fixed combination rules. The experimental results from the score level combination using only one/first training image are illustrated in Figs. 13 and 14. Fig. 13 suggests that the performance from the product and min rule has not been effective in improving the performance. However, the weighted sum rule is quite effective in achieving the performance improvement as can be observed from results in Fig. 14. It can be observed from this figure that the performance improvement from the Haar wavelet and the Log-Gabor filter is significantly higher than those from the DCT and the Log-Gabor filter. Fig. 14(b) summarizes the performance from the combination of DCT scores with those from Log-Gabor using various fixed rules and suggest that even the best results from

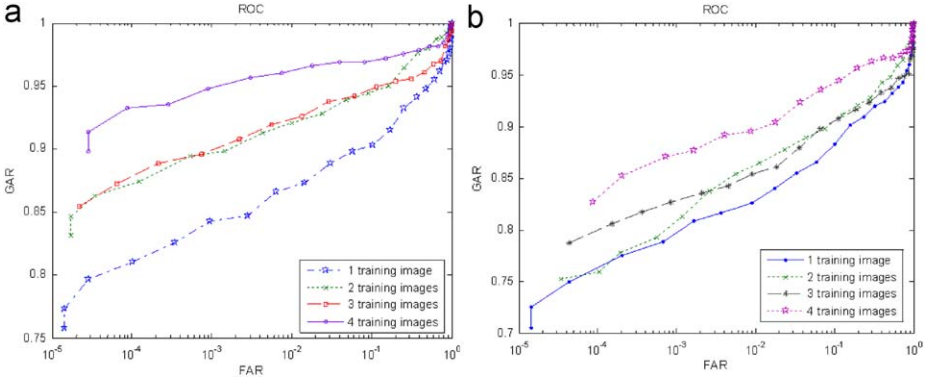

Fig. 11. The ROC from the test data using (a) DCT based and (b) FFT based approach.

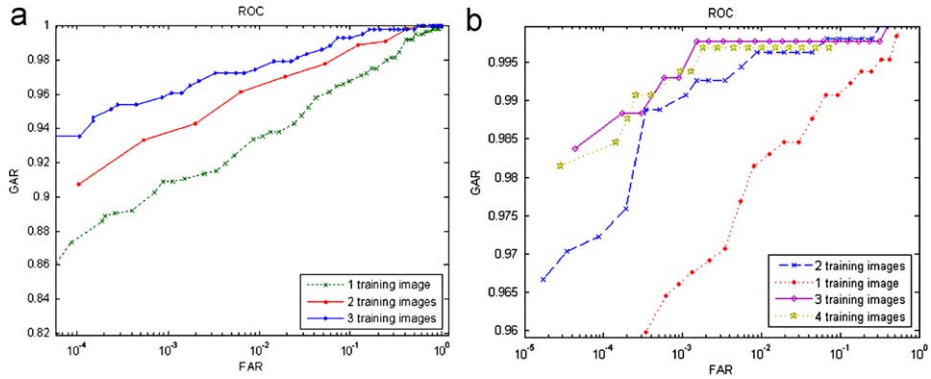

Fig. 12. The ROC from the test data using (a) Haar wavelet and (b) Log-Gabor filter based approach.

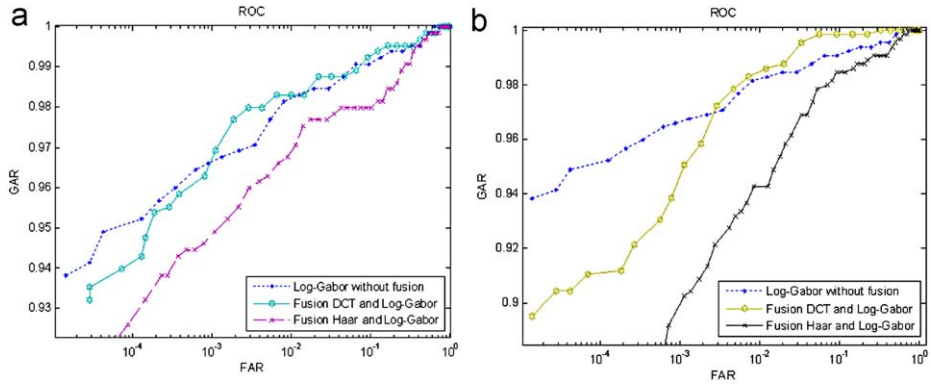

Fig. 13. The fusion of Haar and DCT with Log-Gabor scores using product rule in (a) and Min rule in (b).

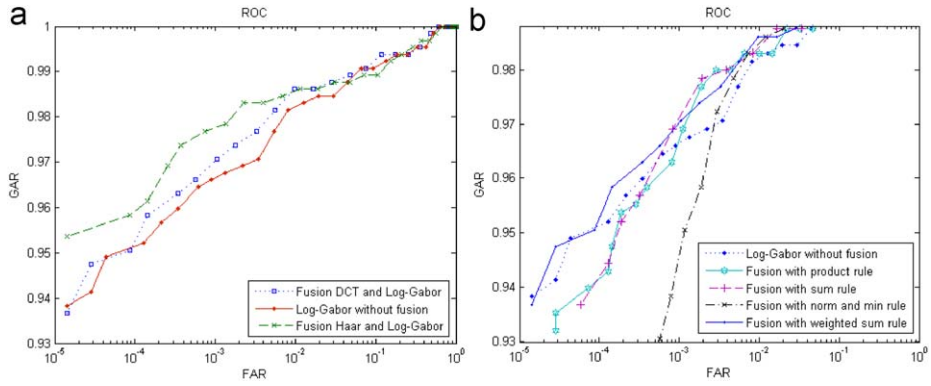

Fig. 14. The ROC using weighted sum rule combination from DCT, Haar and Log-Gabor scores in (a) and comparison of performance from DCT and Log-Gabor using different combination rules in (b).

weighted sum rule does not achieve any appreciable improvement in the performance.

Furthermore, the Haar wavelet approach requires least amount of computations among all approaches and can be implemented with simple integer processing. Therefore, this combination is the most promising to achieve the performance improvement and was further investigated. The equal error rate (EER shown in %) and the decidability index (DI) were used to as the quantitative performance indices to ascertain the performance [22]. Table 1 presents the summary of these performance indices on the CASIA I database. The performance indices in this table suggests significant improvement in the performance while simultaneously combining the scores from the Log Gabor and Haar wavelet based matching.

Table 1
Performance indices from the experiments using CASIA I database.

	One training		Two training	
	EER	DI	EER	DI
Log-Gabor filter	1.62	5.4808	0.55	6.4463
Haar wavelet	4.43	4.6679	2.96	5.3318
Fusion	0.94	5.6948	0.36	6.7175

The proposed approach to achieve the performance improvement was also investigated on CASIA III (lamp) iris image database [14]. We employed 2877 left eye images from all the 411 users to

Table 2
Performance indices from the experiments using CASIA III database.

	EER	DI
Log-Gabor filter	3.72	4.7543
Haar wavelet	13.16	2.8078
Fusion	2.40	4.6993

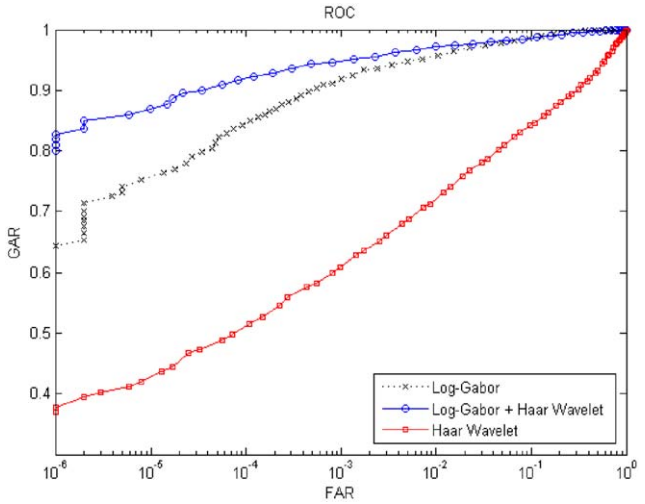

Fig. 15. The performance from CASIA III database using one training image.

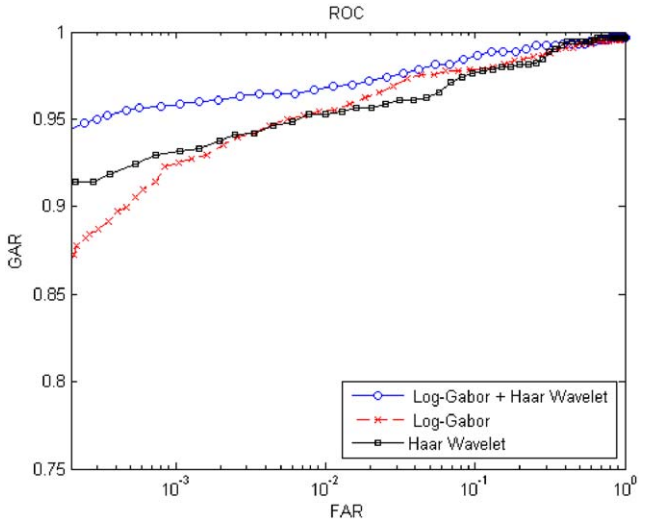

Fig. 16. The performance from IITD database using first/one training image.

ascertain the performance. Our experiments employed first seven images from all 411 users simply to limit the large computations involved in generating imposter scores. The experimental results from the CASIA III database are summarized in Table 2 and also shown in Fig. 15. Each of the ROC's shown in Fig. 14 employed 1,011,060 $(411 \times 410 \times 6)$ imposter matching scores and 2466 (411×6) genuine matching scores. It can be ascertained from ROC in Fig. 15 that the performance improvement, due to the simultaneous usage of Haar wavelet features, is significant. In addition, the IIT Delhi iris database [16] was also used to ascertain the performance improvement. The methods for the performance evaluation on IIT Delhi database were same as used for the CASIA I database. The performance from the IITD database using the one/first training image is shown in Fig. 16. The results illustrate the performance improvement due to the simultaneous usage of Log-Gabor and Haar wavelet features. In order to ascertain the performance improvement from minimum training image, independent of the training image, rigorous experiments were performed to ascertain the average performance. In these set of experiments average of results obtained when each of the eight (five for IITD database) images were employed for training and rest of the images as the test set. The average performance from the IITD database and CASIA I database is summarized in Table 3. The corresponding ROCs are illustrated in Fig. 17. The performance indices presented in Table 3, from this set of experiments, suggest that the achieved performance improvement is quite independent of selected training image. The proposed system is implemented in Visual C++ 6.0 on Windows operating system environment.

Table 3
Performance indices from the average experiments IITD and CASIA I database.

	IITD		CASIA I	
	EER	DI	EER	DI
Log-Gabor filter	2.81	5.7437	2.21	5.2884
Haar wavelet	3.40	6.1762	3.91	4.8016
Fusion	2.59	6.4079	1.48	5.6640

5. Discussion

One of the key challenges in the comparison of performance from the various feature extraction algorithms relates to the selection of the parameters. Therefore, we iteratively selected the different set of parameters, as detailed in Section 2, to achieve the best performance corresponding to the employed database. The CASIA I database is by far the most widely used iris database for the performance evaluation in the literature [7] and has often been cited as standard benchmark for iris algorithms [1]. The recent comments [18] on CASIA I database suggest that images in this dataset have their pupil regions masked to suppress the specular reflections from the near IR illuminators. However, such reflections have been conveniently removed in the pre-processing stage by the inclusion of a median filter as shown in Fig. 6. These reflections are common in CASIA III and IIT Delhi database and thus our implementation does not have any problem in handling pupils with such specular reflections (sample results in Figs. 9 and 10). Therefore, we also investigated the performance on CASIA I database, as this database has been extensively used in several of prior publications, and achieved similar or better performance improvement. The experimental results from the CASIA I database using Gabor filters have also been presented in [5,33]. The experimental results in [5] achieve EER of 0.09% while in [33] the author's have not provided any estimate of EER. However, it is very difficult to compare our results with this work since only a portion of CASIA I database is *publicly* made available and all of which has been employed in our work (while [5,33] utilize full version of this database). The experimental results presented in Tables 1–3 should be seen in the context of single training image and achieved performance can be significantly improved with the increase in number of training images (Table 1).

Our experimental results in Section 4 from the comparison of the four approaches illustrated that the Log-Gabor and Haar wavelet achieves the best performance among the four considered approaches. The performance from Log-Gabor features was best on CASIA I and CASIA III database. However, the achieved performance (Figs. 16 and 17) on IITD database was superior from

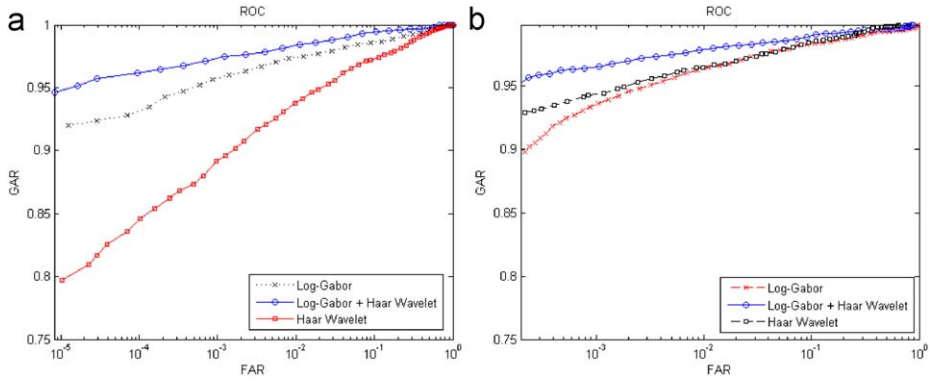

Fig. 17. The average performance from (a) CASIA I and (b) IITD database using one training image.

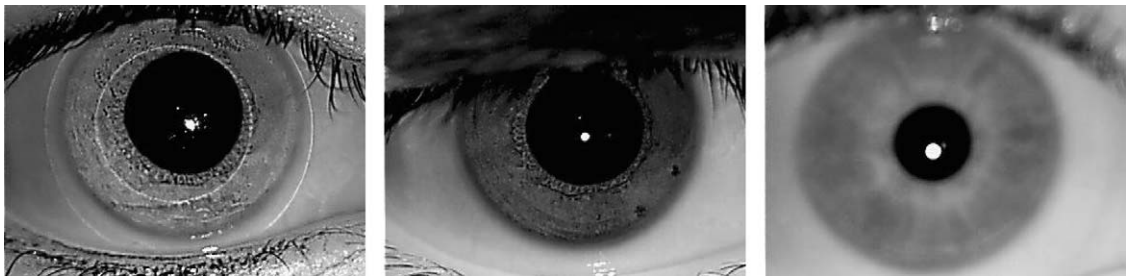

Fig. 18. Some low quality image samples from IITD iris database.

the Haar wavelet features as compared to those from Log-Gabor features. These observations suggest that the performance from the feature extraction algorithms also depend on the employed database (nature of images). Despite the variations in the absolute performance among three databases, the significant performance improvement is consistently observed while combining the scores from the two approaches. The experimental results presented from the CASIA III database, from all 411 users, involved over 12 million ($12 \times 1{,}011{,}060$) comparisons. In our work, we employed first seven images from each of the 411 users, to limit the complexity involved in significantly large number of matching. However, to the best of our knowledge, these results involve the largest number of matching operations yet presented from any *publicly* available iris database.

The observed performance from the IITD database (Figs. 16 and 17) is generally poor, as compared to those from CASIA I and CASIA III database. This could be possibly due to the fact that IITD database contains low-resolution and also poor quality images, as compared to CASIA database. This database employed a low-cost iris camera (370 US$) for imaging and the presence of poor quality iris images can significantly degrade the performance [23] (Fig. 18).

6. Conclusions

This paper has investigated the comparative performance from four different approaches for the iris identification: DCT, FFT, Haar wavelet and Log-Gabor filter. Our experimental results presented in previous section suggest that the performance from the performance from the Log-Gabor filter is the best which is followed by the Haar wavelet, DCT and FFT in order. This paper has also investigated the possible performance improvement using score-level combination. The experimental results suggest that the combination of Log-Gabor and Haar wavelet matching scores using weighted sum rule is the most promising. The Haar wavelet based approach is also the most attractive as it requires minimum computational time and can be easily implemented in fixed point environment. The extensive evaluation of the proposed combination on CASIA I (108 users), CASIA III (411 users) and IITD (224 users) database achieved significant improvement in the performance. The summary of prior work presented in Section 1.2 has suggested that prior efforts have been employing several training images for the performance evaluation. However, the performance evaluation presented in this paper has been focused on usage of one training image.

The motivation for considering only fixed combination rules in this paper was the fact that this approach does not require any training and is computationally simpler. However, the trainable fusion strategies may offer better performance improvement and is suggested for the investigation in the future efforts. The pupil detection algorithm developed in this works well for the three pubic databases used for performance evaluation and assumes that user eyes does not have large specular reflections from the surface of glass that might be present. The presence of large specular reflection and thick black glass frame will limit the accuracy of the performance from the employed iris segmentation approach. Therefore, further efforts are required to develop more accurate iris segmentation method that can be robust to handle such large specular reflection in presence of glasses. Also, this work has been focused on the user authentication and an extension of this work should evaluate the performance for recognition. Even though the speed of developed online system is fast (authenticates individuals in less than a second), we are working to further optimize by using better coding techniques (multi-threaded implementation).

Acknowledgment

This work was partially supported by the research grant from Ministry of Information and Communication Technology,

Government of India, Grant no. 12(54)/2006-ESD. We thankfully acknowledge the Chinese Academy of Sciences Institute of Automation for providing us the CASIA I and CASIA III Iris Image Database.

References

[1] J. Thornton, M. Savvides, B.V.K. Vijay Kumar, A Bayesian approach to deformed pattern matching of iris images, IEEE Trans. Pattern Anal. Mach. Intell. 29 (2007) 596–606.
[2] J. Daugman, High confidence visual recognition of persons by a test of statistical independence, IEEE Trans. Pattern Anal. Mach. Intell. 15 (1993) 1148–1161.
[3] D.M. Monro, S. Rakshit, D. Zhang, DCT-based iris recognition, IEEE Trans. Pattern Anal. Mach. Intell. 29 (2007) 586–595.
[4] W.W. Boles, A security system based on human iris identification using wavelet transform, in: Proceedings of the International Conference on Knowledge-Based Intelligent Electronic Systems, May 1997, pp. 533–541.
[5] L. Ma, T. Tan, Y. Wang, D. Zhang, Efficient iris recognition by characterizing key local variations, IEEE Trans. Image Process. 13 (2004) 739–750.
[6] R.P. Wildes, Iris recognition: an emerging biometric technology, Proc. IEEE 89 (9) (1997) 1348–1363.
[7] H. Proença, L.A. Alexandre, Towards noncooperative iris recognition: a classification approach using multiple signatures, IEEE Trans. Pattern Anal. Mach. Intell. 29 (2007) 607–612.
[8] L. Flom, A. Safir, Iris recognition system, US Patent no. 4 641 394, 1987.
[9] E. Stollnitz, T. DeRose, D. Salesin, Wavelet for Computer Graphics: Theory and Applications, Morgan Kaufmann, Los Altos, CA, 1996.
[10] L. Shinyoung, K. Lee, O. Byeon, Efficient iris recognition through improvement of feature vector and classifier, ETRI J. 23 (2001) 61–70.
[11] C.H. Daouk, L.A. Esber, F.O. Kanmoun, M.A. Alaoui, Iris recognition, in: Proceedings of the ISSPIT, 2002, pp. 558–562.
[12] L. Masek, Recognition of human iris pattern for biometric identification, B.Eng. Thesis, University of Western Australia, 2003. 〈http://www.csse.uwa.edu.au/∼pk/studentprojects/libor/index.html〉, 2008.
[13] P. Yao, J. Li, X. Ye, Z. Zhuang, B. Li, Iris recognition using modified Log-Gabor filters, in: Proceedings of the ICPR 2006, Hong Kong, 2006, pp. 1–4.
[14] D. Fields, Relations between the statistics of natural image and the response properties of cortical cells, J. Opt. Soc. Am. 4 (12) (1987) 2379–2394.
[15] CASIA IRIS Database, 〈http://www.cbsr.ia.ac.cn/english/IrisDatabase.asp〉, 2008.
[16] IITD Iris Database, 〈http://web.iitd.ac.in/∼biometrics/Database_Iris.htm〉, 2008.
[17] D.M.J. Tax, M.V. Breukelen, R.P.W. Duin, J. Kittler, Combining multiple classifiers by averaging or combining, Pattern Recognition 33 (2000) 1475–1485.
[18] P.J. Phillips, K.W. Bowyer, P.J. Flynn, Comments on the CASIA version 1.0 iris dataset, IEEE Trans. Pattern Anal. Mach. Intell. 29 (2007) 1869–1870.
[19] 〈http://www.jiristech.com/english/products/iris.php〉, 2008.
[20] J. Huang, T. Tan, L. Ma, Y. Wang, Phase correlation based iris image registration model, Comput. Sci. Technol. 20 (3) (2005) 419–425.
[21] J. Daugman, Probing the uniqueness and randomness of IrisCodes: results from 200 billion iris pair comparisons, Proc. IEEE 94 (11) (2006) 1927–1935.
[22] J. Daugman, How Iris recognition works, IEEE Trans. Circuits Systems Video Technol. 14 (2004) 21–30.
[23] Y. Chen, S. Dass, A.K. Jain, Localized iris image quality using 2-D wavelets, in: Proceedings of the ICB, Hong Kong, 2006, pp. 373–381.
[24] L. Ma, T. Tan, Y. Wang, D. Zhang, Local intensity variation analysis for iris recognition, Pattern Recognition 37 (6) (2004) 1287–1298.
[25] K.W. Bowyer, K. Hollingsworth, P. Flynn, Image understanding for iris biometrics: a survey, Comp. Vision and Image Understanding 110 (2008) 281–307.
[26] X. He, P. Shi, A new segmentation approach for iris recognition based on hand-held capture device, Pattern Recognition 40 (4) (2007) 1326–1333.
[27] W.K. Kong, D. Zhang, Detecting eyelash and reflection for accurate iris segmentation, Int. J. Pattern Recognition 17 (6) (2003) 1025–1034.
[28] L. Yu, D. Zhang, K. Wang, The relative distance of key point based iris recognition, Pattern Recognition 40 (2) (2007) 323–430.
[29] A. Kumar, A. Passi, Comparison and combination of iris matchers for reliable personal identification, Proc. CVPR 2008, Anchorage, Alaska, USA, 2008, pp. 21–27.
[30] C. Sanchez-Avila, R. Sanchez-Reillo, Two different approaches for iris recognition using Gabor filters and multiscale zero-crossing representation, Pattern Recognition 38 (2) (2005) 231–240.
[31] B. Ulery, A.R. Hicklin, C. Watson, W. Fellner, P. Hallinan, Studies of biometric fusion, NIST Technical Report no. IR 7346, September 2006.
[32] K. Nandakumar, Y. Chen, S.C. Dass, A.K. Jain, Likelihood ratio based biometric score fusion, IEEE Trans. Pattern Anal. Mach. Intell. 30 (2008) 342–347.
[33] L. Ma, T. Tan, Y. Wang, D. Zhang, Personal identification based on iris texture analysis, IEEE Trans. Pattern Anal. Mach. Intell. 25 (2003) 1519–1533.

About the Author—AJAY KUMAR received the Ph.D. degree from The University of Hong Kong in May 2001. He was with the Indian Institute of Technology Kanpur and at Indian Institute of Technology Delhi, before joining the Indian Railway Service of Signal Engineers (IRSSE) in 1993. He completed his doctoral research at The University of Hong Kong in a record time of 21 months (1999-2001). He worked a postdoctoral researcher in the Department of Computer Science, Hong Kong University of Science and Technology (2001-2002). He was awarded The Hong Kong Polytechnic University Postdoctoral Fellowship 2003–2005 and worked in the Department of Computing. He has been an Assistant Professor in the Department of Electrical Engineering, Indian Institute of Technology Delhi (2005–2008). He has been the founder and lab in-charge of Biometrics Research Laboratory at Indian Institute of Technology Delhi. Since 2009, he has now been working as an Assistant Professor in the Department of Computing, The Hong Kong Polytechnic University, in Hong Kong. His research interests include pattern recognition with the emphasis on biometrics and computer-vision based defect detection.

About the Author—ARUN PASSI received Dual Degree (B.Tech and M.Tech) in Electrical Engineering from Indian Institute of Technology, Delhi in 2007. He joined Biometrics Research Laboratory in August 2006 and has since been working towards his dual degree major project. His research interest include biometrics with the emphasis on iris recognition.